

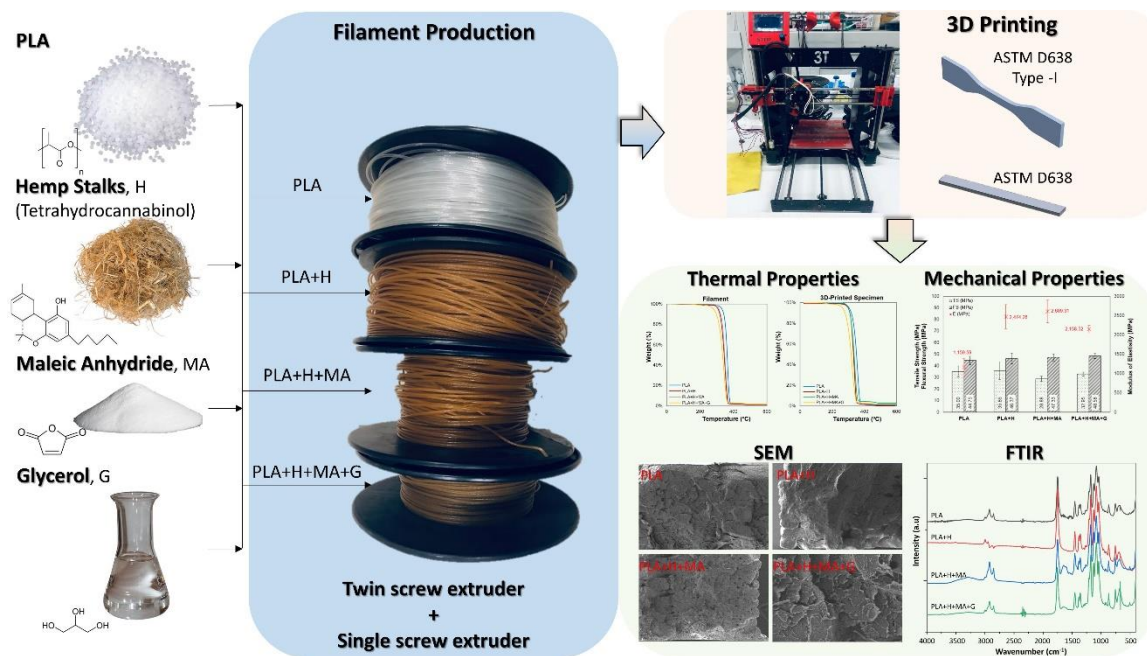
# 3D-Printed Biocomposites from Hemp Fibers Reinforced Polylactic Acid: Thermal, Morphology, and Mechanical Performance

Esra Celik <sup>a</sup>, Mesut Uysal <sup>a,b,\*</sup>, Omer Yunus Gumus <sup>c</sup> and Cagatay Tasdemir <sup>a,b</sup>

\*Corresponding author: [mesut.uysal@btu.edu.tr](mailto:mesut.uysal@btu.edu.tr)

DOI: 10.15376/biores.20.1.331-356

## GRAPHICAL ABSTRACT



# 3D-Printed Biocomposites from Hemp Fibers Reinforced Polylactic Acid: Thermal, Morphology, and Mechanical Performance

Esra Celik <sup>a</sup>, Mesut Uysal <sup>a,b,\*</sup>, Omer Yunus Gumus <sup>c</sup> and Cagatay Tasdemir <sup>a,b</sup>

Thermal, morphological, and mechanical properties were studied for 3D-printed biocomposites prepared from polylactic acid (PLA) and hemp fibers. For this purpose, the neat PLA, PLA/Hemp fiber (3 wt%), PLA/Hemp fiber/Maleic anhydride (3 wt% and 0.6 wt%), and PLA/Hemp fiber/Maleic anhydride/Glycerol (3 wt% and 0.6 wt% + Glycerol added in 10% of PLA) biocomposites were extruded to obtain filaments for fused filament fabrication (FFF). Thermogravimetric analysis (TGA) provided temperatures corresponding to 5%, 10%, and 90% mass losses for materials before and after 3D printing. During 3D printing, filaments were extruded with a nozzle temperature of 220 °C; consequently, their thermal properties worsened after 3D printing. In thermal analysis,  $T_g$  increased by adding hemp fiber and maleic anhydride but was decreased with glycerol addition. The tensile and flexural strengths of neat PLA and biocomposites were not statically different, but flexural strength was slightly increased by adding ingredients one by one. Regarding modulus of elasticity (MOE) of materials, the sample group of the PLA/hemp fiber/maleic anhydride had the highest value. However, glycerol addition decreased MOE by 17%. These results showed that material performance of the PLA could be improved or remain statistically identical by adding hemp fiber, maleic anhydride, and glycerol.

DOI: 10.15376/biores.20.1.331-356

Keywords: 3D printing; PLA; Hemp fiber; Natural fiber-based composite; Biocomposite

Contact information: a: Bursa Technical University, Department of Biocomposite Engineering, Bursa 16310, Türkiye; b: Bursa Technical University, Department of Forest Industry Engineering, Bursa 16310, Türkiye; c: Bursa Technical University, Department of Polymer Materials Engineering, Bursa 16310, Türkiye; \*Corresponding author: mesut.uysal@btu.edu.tr

## INTRODUCTION

Additive manufacturing (AM) or 3D printing has revolutionized various industries by enabling the creation of complex structures with customizable properties and cost-effective layer-by-layer manufacturing (Zindani and Kumar 2019; Jiang *et al.* 2020). Reinforced polymers in 3D printing have become important due to environmental issues such as climate change that have brought vital variations in the industry. Manufacturers have been adjusting their production management and organization according to the environmental impacts of their production process, inputs in the production, and by-product, semi-product, and final product formations. Therefore, the materials utilized in the production are specifically eco-friendly and provide serviceability during usage *via* their mechanical, morphological, and thermal properties (Mantelli *et al.* 2022). According to ASTM F2792 (2012), 3D printing is classified into seven categories; namely, binder

jetting, directed energy deposition, material extrusion, material jetting, powder bed fusion, sheet lamination, and vat photopolymerization (Shahrubudin *et al.* 2019). Polymer-based materials are utilized in the material extrusion category, which is also called fused deposition modeling or fused filament fabrication (FFF). In the FFF, thermoplastic filaments are heated and melted during extrusion *via* a nozzle tip, and geometry is shaped layer by layer. The FFF is the most popular technology, and plastics are the most utilized materials in 3D printing. According to Muthe *et al.* (2022), the number of studies related to FFF technology has been twice as high compared to stereolithography (SLA) in recent years, and 46% of companies used FFF printers in 2018. In addition, plastic was the preferred material compared to metals and resins, and standard polylactic acid (PLA) was the most used polymer worldwide. The PLA, which is a bio-derived material, is followed by polyhydroxyalkanoates (PHA), polyethylene (PE), polyethylenefurandicarboxylate (PEF), polycarbonate (PC), and polyamide (PA) as bio-derived materials. Among all, PLA was the most preferred due to its higher tensile and flexural strengths compared to others. PLA belongs to an aliphatic polyester group, and its polycondensation yields a low molecular weight polymer; that is, it shows relatively weak mechanical properties (Sodergard and Stolt 2002; Mehrpouya *et al.* 2021; Nkuna *et al.* 2024). Lactic acid has a chiral carbon atom in its molecular structure and has D- and L-lactic acid enantiomers; namely, they are called poly (D-lactic acid) (PDLA) and poly(L-lactic acid) (PLLA). PLLA has been shown to have a higher performance compared to PDLA due to stereoisomerism in PLA (DeStefano *et al.* 2020; Nkuna *et al.* 2024). Moreover, the L-isomer for PLA is preferred for 3D printers because of its favorable printability. However, in some cases, neat PLA does not provide sufficient material properties, so it is reinforced with fibers obtained naturally or synthetically to improve the material process and sustainability and reduce material and production costs and environmental impact (Mukherjee and Kao 2011; Getme and Patel 2019; Wickramasinghe *et al.* 2020). Wood, kenaf, jute, flax, hemp, and harakeke are primarily used natural fibers as filler materials in the filaments in 3D printing. Moreover, cellulose, acetylated tannin, and cork have been included as fillers in PLA-based biocomposites. Moreover, food waste (Ali *et al.* 2024) and seashells (Martinovic *et al.* 2024) were also used as fillers in biocomposites.

Lignocellulose-based biocomposites are preferable because of environmental concerns and provide better mechanical performance due to a greater length-to-diameter ratio. Cellulose content and microfibril angle play critical roles in the mechanical properties of natural fibers; correspondingly, fibers with higher mechanical properties provide better performance for biocomposites (Mukherjee and Kao 2011; Ilyas *et al.* 2021). Additionally, the surface structure of natural fibers plays a critical role in the adhesion of fiber and matrix material in biocomposites. However, natural fibers have a drawback due to hydrophilicity, which causes weak adhesion between fiber and matrix (Ilyas *et al.* 2021). The material strength may not continuously increase due to a decrease in hydrogen bonds between cellulose and a weak interaction between cellulose and PLA (Zhou *et al.* 2021). Maleic anhydride, alkali, and stearic acid are treatments that can create bonding between free hydroxyl groups of fiber and the ester linkage of the matrix (Lv *et al.*, 2016). Alkali-treated hemp fiber and PLA biocomposites were found to provide higher mechanical strength compared to those of the non-treated (Baghaei *et al.* 2014; Arockiam *et al.* 2021). Plasticizers, such as glycerol and tributyl citrate, are also used in biocomposites to increase the dispersion and interaction between fiber and matrix (Xie *et al.* 2017; Almeida *et al.* 2024).

The fiber particle size matters because of the nozzle diameter, which could extrude biocomposites. 3D-printed biocomposites with a rice straw fiber particle size of 125  $\mu\text{m}$  provided better mechanical properties than those of 250  $\mu\text{m}$ . Moreover, the particle sizes of 74 and 97  $\mu\text{m}$  might cause an unwanted extrusion agglomeration and a possible printing defect (Yu *et al.* 2021). Sufficient particle size provides adequate interfacial adhesion between fiber and matrix, so higher mechanical performance can be achieved. Le Duigou *et al.* (2019) made continuous flax/PLA filaments *via* a coating continuous fiber fabrication process and printed longitudinal ( $0^\circ$ ) and transverse ( $90^\circ$ ) oriented tensile test specimens. Their tensile strength was 4.5 and 10 times greater than neat PLA and discontinuous fiber-reinforced PLA, respectively. Kajbič *et al.* (2023) stated that an increase in the number of fibers for continuous flax fiber reinforced significantly improved material strength. In contrast, an increase in the number of flax fibers in biocomposite after a certain number causes a reduction in material strength (Paulo *et al.* 2023). Similarly, Yang *et al.* (2021) observed that adding poplar fiber by 5 wt% to PLA increased the flexural strength and modulus, whereas those of 7 wt % and 9 wt % subsequently decreased flexural properties.

Mazur *et al.* (2022) stated that the mechanical strength of neat PLA was higher compared to those of PLA/wood, PLA/bamboo, and PLA/cork. The addition of natural fibers to PLA slightly enhanced the degree of crystallinity. 3D-printed PLA bamboo fiber-based biocomposites had lower thermal conductivity than wood (Takagi *et al.* 2007). PLA/wood-based biocomposite must be extruded at significantly higher temperatures than the PLA melting point to achieve sufficient interfacial adhesion (Luedtke *et al.* 2019).

Kananathan *et al.* (2022) examined various infill patterns and densities for PLA/coconut wood biocomposites. In the tensile test, the highest strength was obtained with a concentric infill pattern, while those giving the highest compression strength were of grid infill. Furthermore, increasing infill density (25% to 50%) increased material strength for all patterns. Guessasma *et al.* (2022) stated that vertical building orientation reduced the tensile strength and elasticity of the polymers, and the printing direction, along with the sample, provided higher strength for 3D-printed polymers. Bragaglia *et al.* (2023) concluded that the tensile strength of the 3D-printed PLA decreased by 70 to 75% with changing raster orientations from  $0^\circ$  to  $90^\circ$  due to the interaction between printing direction and the layerwise nature of the printed polymers. Lares Carrillo *et al.* (2023) compared the tensile strength of the PLA and PLA/wood and concluded that 3D-printed PLA with raster orientations  $0^\circ$ ,  $45^\circ$ , and  $90^\circ$  had 28% to 34% higher strength than those comprising PLA/wood. Moreover, 3D-printed parts with a raster orientation of  $0^\circ$  had the highest tensile strength, followed by those of  $45^\circ$ . Ambade *et al.* (2023) stated that an increase in infill density and nozzle temperature (190 to 230  $^\circ\text{C}$ ) increased 3D-printed materials, but an infill pattern with an infill density of 100% was not significantly different. Sultana *et al.* (2024) stated that layer height had the highest effect on the mechanical properties of 3D-printed PLA/wood biocomposite, followed by nozzle temperatures, infill density, and printing speed. Mishra *et al.* (2024) studied the effects of infill pattern, infill density, printing speed, and layer height of 3D-printed wood/PLA biocomposite. They stated that layer heights of 0.25 and 0.3 mm had higher tensile and flexural strengths, while lower printing speed and higher infill rate increased these strengths. In addition, the cubic infill pattern provided the highest strength for tensile strength, whereas those of tri-hexagon had the highest flexural strength.

Agricultural waste has also been evaluated in 3D-printed biocomposites. Jałbrzykowski *et al.* (2022) investigated the effects of onion and buckwheat husk/PLA with

10, 20, and 30 wt%. Increasing the amount of fillers decreased the tensile strength of the biocomposites up to 14% to 40%. Arumaiselvan *et al.* (2024) examined the effect of adding *Cryptostegia grandiflora* fibers to PLA and increased tensile strength by 33.5%, flexural strength by 14.1%, and thermal degradation by 15%. Likewise, Xiao *et al.* (2019) stated that the tensile and flexural strength of PLA/Hemp fiber was reduced by adding hemp fibers at levels of 10, 20, 30, and 40 wt%. However, its elasticity increased up to 30 wt%, and then was reduced at 40 wt%. Wang *et al.* (2024) compared the 3D-printed biocomposites made of PLA/hemp shives, PLA/tomato, PLA/hemp bud, and PLA/pruned orange trees. The results showed that the PLA/hemp shives biocomposite had the highest tensile strength, followed by PLA/hemp bud—the tensile strengths of the biocomposites reduced with increasing raster orientation from 0° to 90°. Similarly, Antony *et al.* (2020) stated that the tensile strength of PLA/Hemp (20 wt% to 25 wt%) decreased with raster orientation from 0°/90° to 45°/-45°. Cali *et al.* (2020) emphasized that adding hemp and weed increased the elasticity of neat PLA but reduced melting temperature. Arnold and Smith (2021) examined treatment effects on material properties of the 3D-printed PLA/hemp fiber biocomposites and concluded that adding hemp fibers to PLA reduced its flexural strength and elasticity. Sodium hydroxide treatment increased these properties compared to non-treated, but flexural strength and elasticity decreased by adding triethoxysilane to sodium hydroxide solution for surface treatment. Moreover, adding hemp fiber to PLA showed moderate changes in glass transition and melting temperatures. Dogru *et al.* (2021) studied the effect of aging and infill patterns on the mechanical properties of PLA/hemp fiber (10 wt%) biocomposites. Grid infill patterns gave higher tensile strength than concentric patterns, which was decreased by aging 3D-printed PLA/hemp fiber.

Moreover, the circular economy has recently attracted attention because of its potential for sustainable development. It aims to increase resource utilization with higher efficiency by reducing the environmental impact of materials. Bianchi *et al.* (2022) compared the global warming potential for glass fiber-reinforced polyamide and hemp fiber-reinforced PLA (20 wt%). Results showed that PLA/hemp fiber showed 38% less environmental impact than glass-reinforced PLA. Hemp harvest has recently increased in Türkiye, and its agricultural waste should be evaluated in value-added products. According to the Food and Agricultural Organization (FAO), the harvested area for hempseed was 10 ha in 2020 and increased to 194 ha in 2022. It shows that an increase in the harvested area for hempseed would increase the amount of harvested hemp stalks, correspondingly increasing the waste of hemp stalks. Therefore, the use of hemp stalks, in particular, has been on the rise, reflecting the industry's increasing interest in sustainable and versatile materials. Furthermore, hemp could be harvested after 4 months of cultivation which is a short time compared to wood.

This study aimed to investigate the thermal, morphological, and mechanical properties of 3D-printed biocomposites made of PLA/hemp fibers. In doing so, it was examined how the presence of hemp fiber, hemp fiber/maleic anhydride, and hemp fiber/maleic anhydride/glycerol in PLA changed these properties. Thermogravimetric analysis (TGA) and differential scanning calorimetric (DSC) analysis were performed. Fourier Transform Infrared Spectroscopy (FTIR) analysis was made to identify functional groups in biocomposites. Flexural strength, modulus of elasticity (MOE), and tensile strength of the neat PLA and biocomposites were assessed for mechanical properties. Lastly, fracture surfaces were analyzed using scanning electron microscopy (SEM).

## EXPERIMENTAL

### Materials and Compounding of Biocomposites

Hemp (*Cannabis sativa* L.) stalks were procured from the Samsun region of Türkiye and used as filler material. *Cannabis sativa* is a well-known source of higher tetrahydrocannabinols (THC) variant but contains less than 0.3% THC, so it can be used numerous applications (Edyta *et al.* 2015; Fike 2016; Naithani *et al.* 2020). Polylactic acid (PLA, Luminy/L175) granules were used as matrix material. Maleic anhydride (MA, Merck/for synthesis) as a compatibility material and glycerol (G, Carlo Erba Reagents30 Be, Vegetal origin) as a plasticizer to reduce the fragility of the filament, were also included. Table 1 shows the ratio of the components in the sample groups. These ratios in the design of experiment were obtained methodically and adjusted until they successfully produced filaments. The higher ratio of the hemp fiber increased the fragility of the filaments.

**Table 1.** Ratios of the Components in Bioplastic and Biocomposite Materials

Sample Group	PLA (wt%)	Hemp fiber (wt%)	Maleic Anhydride (wt%)	Glycerol (wt%)*
PLA	100	-	-	-
PLA+H	97	3	-	-
PLA+H+M	96.4	3	0.6	-
PLA+H+M+G	96.4	3	0.6	9.64*

\* Glycerol was added to the mixture, in amount of 10% of PLA

In the first stage of preparing the hemp fiber (H), the hemp stalks were coarsely ground in the Wiley mill to 500 µm and finely ground in the IKA MF 100 mill. The ground hemp stalks were passed through the shaking sieve, and the fiber that remained under the 75 µm (~200 mesh) sieve was collected for the biocomposites. In the second stage, the PLA+H mixtures were physically combined to create a total mixture of 250 g. MA is commonly used as compatibilizer for composites of PLA/cellulose based materials due to its low toxicity (Zhou *et al.* 2018). For the PLA+H+MA mixture, the H was firstly modified with MA by solvent-free method according to a modified procedure in the literature (Li *et al.* 2017). The chemical modification was carried out by ring opening esterification of MA with the free hydroxyl groups of H. To do so, the H and MA were mixed then the mixture was kept in an oven at 70 °C for at least 24 h. After this treatment, H+MA was physically combined with PLA to create 250 g mixtures. All mixtures were then kept in an oven at 70 °C for at least 24 h to remove moisture before proceeding to the extrusion process. The purpose of the 250 g mixtures was to provide consistency for the amount of PLA and H during feeding in the extruder because the sizes of the PLA granules and H particles were not identical. As a plasticizer, glycerol was added to the mixtures of PLA+H+MA before the twin-screw extruder process, and then the extruder was fed with the mixture of PLA+H+MA+G. In the literature, there are many studies reporting on the usage of glycerol as a plasticizer for both PLA and cellulose based materials (Tarique *et al.* 2021; Halloran *et al.* 2022)

In the *twin-screw extruder* process, the mixtures taken from the oven were then melt-mixed in a Polmak Plastic/Lab 18-mm twin-screw extruder to produce the composites. Temperatures of 90 – 130 – 175 – 185 – 185 -190 – 190 – 185 – 180 – 180 – 165 °C were used in the extruder from the feeding zone to the end. The reasons for using

different temperatures in the twin-screw extruder were to ensure that the torque generated by the screw rotation speed of 20 rpm did not exceed 30% when pushing the material. This would maintain a higher viscosity of the molten samples coming out of the extruder, thereby preserving the continuous strand form. After cooling from cold water tank, the strand of the biocomposites was converted into granules. To remove moisture, all granules were kept in the oven at a temperature of 70 °C for at least 24 h before proceeding to the single-screw extruder process.

In the *single-screw extruder process*, a Polmak Plastic/Lab 18-mm single-screw extruder was used to produce filament for 3D printers with a diameter of 1.75 mm. Temperatures of 170 – 175 – 180 °C were used in the heating zones with a temperature of 50 °C for a hot water tank. Speeds of extruder and traction were adjusted during extrusion to keep the diameter of the filaments at  $1.75 \pm 0.1$  mm. To remove moisture, all filaments were kept in the oven at a temperature of 50 °C for at least 24 h before proceeding to the 3D printing process.

### Additive Manufacturing

The filaments obtained in a form suitable for 3D printing were used to manufacture tensile and bending specimens, modeled according to ASTM D638 (2010) and ASTM D790 (2010) standards, respectively, using AutoCAD software (Autodesk, v.2023, San Francisco, CA, USA). The G-codes required for 3D printers were generated with the Cura 4.8 software (Ultimaker, Utrecht, Netherlands), where the production parameters were created. These printing parameters are given in Table 2.

**Table 2.** Additive Manufacturing Parameters Used in 3D Printing

Parameters	Description
Nozzle temperature	220 °C
Bed temperature	70 °C
Nozzle diameter	0.6 mm
Layer thickness	0.3 mm
Fill rate	100%
Fill pattern	Rectilinear
Flow rate	100%
Printing speed	100 mm/min
Raster orientation	-45°/+45°

### Thermogravimetric Analysis

Thermogravimetric analysis was used to determine the degradation temperatures and rates of polymers and to identify the amount of volatile material, additives, and reinforcing materials they contain (BS EN ISO 11358-1 2014). This study used TGA to determine the degradation temperatures and thermal stability of the extruded bioplastic and biocomposite materials. A Hitachi Hi-Tech STA7200 TGA (Hitachi High-Tech Technologies Corporation, Tokyo, Japan) device was used. The specimens were placed in pans and weighed on the device's precision balance. The initial weight of the samples was recorded, and then they were sent to the TGA furnace. During the TGA process, the temperature was increased from 25 to 900 °C at a heating rate of 10 °C/min under a nitrogen atmosphere. After the test, the degradation temperatures at 5%, 10%, and 90% mass loss and the maximum degradation rates were determined. TGA analysis was performed on filaments and 3D-printed specimens for each sample group to determine the thermal degradation after single screw extrusion process and 3D printing, respectively.

### Differential Scanning Calorimeter Analysis

According to BS EN ISO 11357-3 (2021) and BS EN ISO 11357-4 (2021) standards, the thermal analysis of the composite was performed to determine the glass transition temperature ( $T_g$ ), melting and crystallization temperatures, and enthalpy measurements using DSC. For each sample group, 10 mg samples attained from filaments after single screw extrusion process were used. The tests were conducted under a nitrogen atmosphere using a TA SDT 650 (TA Instruments, New Castle, DE, USA). The filaments were tested using a heating, cooling, and heating cycles (20 °C – 200 °C – 20 °C) at a heating rate of 10 °C/min. For the polymeric materials that undergo several thermal processes, in order to investigate pure properties, the thermal history was eliminated by an initial heating. For the case of this study, as the water tank cooling was used in the filament production process, any possible semi-stable phase or uncompleted crystallization because of the fast cooling may be detected in the first heating. On the other hand, since there is not any cooling during 3D-printing, slow cooling is the case which is similar to the cooling step in the DSC, so the second heating may be considered to simulate the 3D-printed samples. The thermal properties of the filament were analyzed during the first heating process. In contrast, the thermal behaviors during the second heating process simulated the thermal processes the filament would be exposed to during 3D printing. The  $T_g$ , cold crystallization temperature ( $T_{cc}$ ), and melting temperature ( $T_m$ ) were recorded. The crystallinity degree ( $X_c$ , %) of the PLA phase was calculated using Eq. 1 (Xiao *et al.* 2019),

$$X_c = \frac{(\Delta H_m - \Delta H_{cc})}{\Delta H_m^* \times w} \times 100 \quad (1)$$

where  $\Delta H_m$  is the melting enthalpy,  $\Delta H_{cc}$  is the cold crystallization enthalpy,  $\Delta H_m^*$  is the melting enthalpy for 100% crystalline PLA (93 J/g), and  $w$  is the weight fraction of PLA in the biocomposite material (g).

### Fourier Transform Infrared Spectroscopy Analysis

Fourier Transform Infrared Spectroscopy is a widely used technique to identify functional groups within materials (solid, liquid, and gas) using infrared radiation (Khan *et al.* 2018). The functional groups in the produced samples were determined using a Bruker Tensor 37 (Bruker, Billerica, MA, USA) device with an Attenuated total reflectance (ATR) module. Measurements were taken in the wavenumber range of 4000 to 400  $\text{cm}^{-1}$ , with a resolution of 4  $\text{cm}^{-1}$ , and 32 scans. The spectra were evaluated using Bruker OPUS software.

### Determination of Flexural Properties

Specimens for the flexural strength and modulus of the bioplastic and biocomposite materials were prepared according to the ASTM D790 (2010) standard (Type-I) and tested using a Shimadzu AG-IC universal testing machine. The specimens were subjected to a static vertical load at a rate of 5.2 mm/min (Fig. 1). After the loading reached the ultimate load on the specimens, the test was continued until the load decreased to 80% of this ultimate value. The result of the experiment was load-deformation curves. Using these curves, the flexural strength ( $\sigma_F$ , MPa) and the flexural modulus ( $E$ , MPa) of the specimens were calculated according to Eqs. 2 and 3, respectively,

$$\sigma_F = \frac{3 \times F_{ult} \times l}{2 \times w \times t^2} \quad (2)$$

where  $F_{ult}$  is the ultimate load (N),  $l$  is the span (mm),  $w$  is the width of the specimen (mm), and  $t$  is the thickness of the specimen (mm). Flexural modulus was calculated following Eq. 3,

$$E = \frac{\Delta F \times l^3}{4 \times \Delta d \times w \times t^3} \quad (3)$$

where  $\Delta F$  is the difference between two load levels retrieved from the linear region of the load-deformation curve (N), and  $\Delta d$  is the difference of deformations at the  $\Delta F$  (mm).

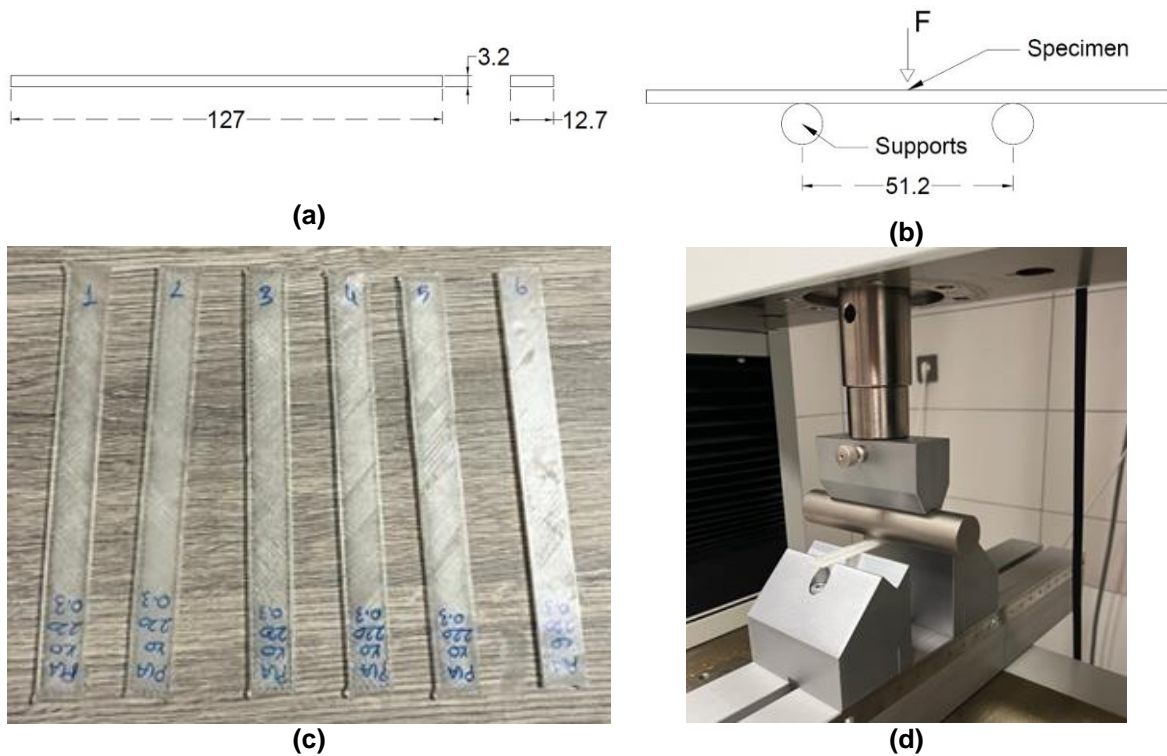


**Fig. 1.** (a) Configuration of the three-point bending test specimen (mm); (b) Three-point bending test configuration (mm); (c) Tested specimens ; and (d) Three-point bending test

### Determination of Tensile Strength

The specimens for tensile strength of bioplastic and biocomposite materials were prepared according to ASTM D638 (2010) standard (Type-I) and tested using a Shimadzu AG-IC Universal testing machine (Fig. 2). The specimens were exposed to static load applied parallel to the axis at a loading rate of 5 mm/min, as indicated in Fig. 2c. The loading was continued until the fracture load was reached on the specimens, and load-deformation curves were obtained. Using these curves, the tensile strength ( $\sigma_T$ , MPa) of the specimens was calculated according to Eq. 4,

$$\sigma_T = \frac{F_{ult}}{w \times t} \quad (4)$$

where  $F_{ult}$  is the ultimate load (N),  $w$  is the width of the specimen (mm), and  $t$  is the thickness of the specimen (mm).

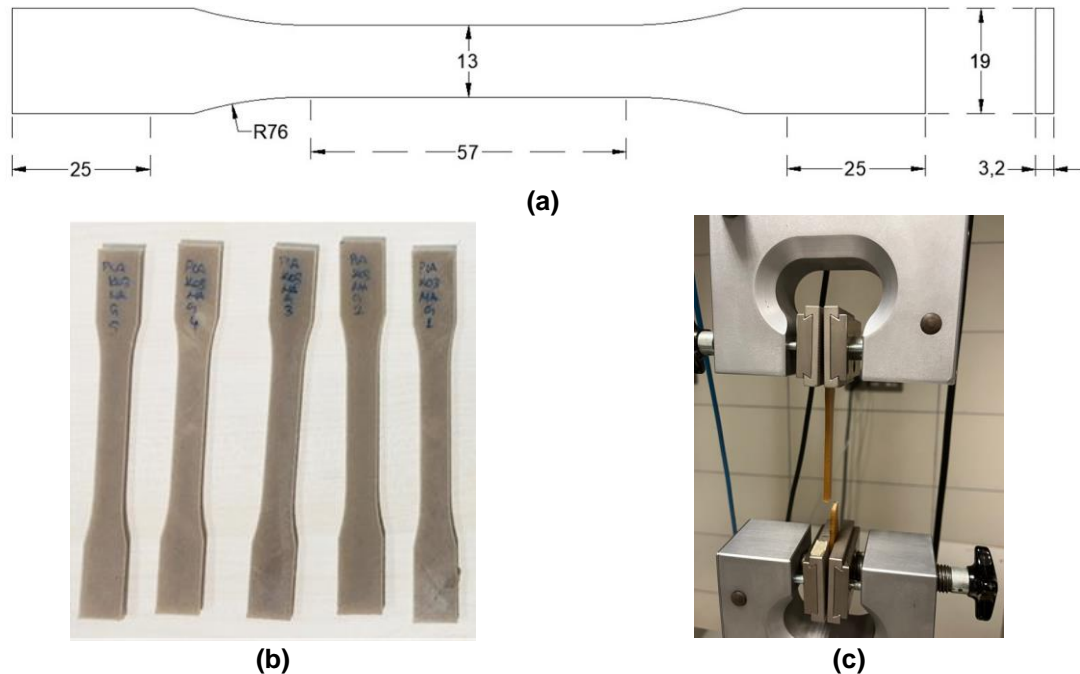


**Fig. 2.** (a) Configuration of the tensile test specimen (mm); (b) Tested specimens; and (c) Tensile test

### Examination of Fracture Surfaces Using Scanning Electron Microscopy

Fracture surfaces will be examined using SEM. The Carl Zeiss/Gemini 300 (ZEISS Group, Oberkochen, Germany) device was used for this experiment. A thermal electron source was employed, and an acceleration voltage of 3.0 kV was preferred (Yang and Yeh 2020). Before analysis, samples taken from the fracture surfaces of tensile specimens were coated with a platinum and gold mixture in Leica/ACE600 device (Leica Microsystems, Wetzlar, Germany).

### Statistical Analysis

The flexural strength and modulus of the bioplastic and biocomposite materials obtained in the three-point bending tests, as well as those of tensile strength obtained in the tensile tests, were analyzed for statistical significance using one-way analysis of variance (ANOVA) and Tukey comparison analyses in Minitab statistical analysis software (Minitab LLC, 18, State College, PA, USA). The effects of independent variables on these mechanical properties of the materials were also interpreted using interaction and main effect plots.

## RESULTS AND DISCUSSION

### Thermal Properties of PLA and Biocomposite Materials

The TGA results obtained from analysis on PLA and biocomposite materials before and after 3D printing are presented in Fig. 3 and Table 3. The filament made of PLA was degraded 5%, 10% and 90% mass losses at 331.5, 342.0, and 374.7 °C, respectively. 3D printed PLA specimens had the lower degradation temperature for 5% (303.7 °C) and 10% (318.6 °C) mass losses but slightly higher for 90% (368.4 °C) mass losses. Adding hemp

to PLA, decreased degradation temperature for both filament and 3D-printed specimens. 5% mass losses occurred at 307.5 °C while those of 10% and 90% were at 318.2 and 361.2 °C, respectively. 3D-printed PLA+H specimens showed 9 to 14 °C lower thermal degradation than PLA+H filaments. Doğru *et al.* (2022) observed the decreases in thermal degradation by adding hemp to PLA due to lower thermal degradation of the hems compared to PLA. Adding MA to PLA+H biocomposites increased the degradation temperature by 3 to 4 °C for filaments while there were slight changes in the degradation temperature for 5% and 10% mass losses but those of 90% were increased 6.76 °C. Lv *et al.* (2016) reported that adding MA to wood reinforced PLA increased the degradation temperature but not higher than neat PLA. The addition of glycerol to the PLA+H+MA biocomposite material resulted in a significant decrease in degradation temperature, which can be attributed to the lower thermal stability of glycerol compared to the other components in the composites. The nozzle temperature applied during the 3D printing process affected the thermal properties of the bioplastic and biocomposite materials.

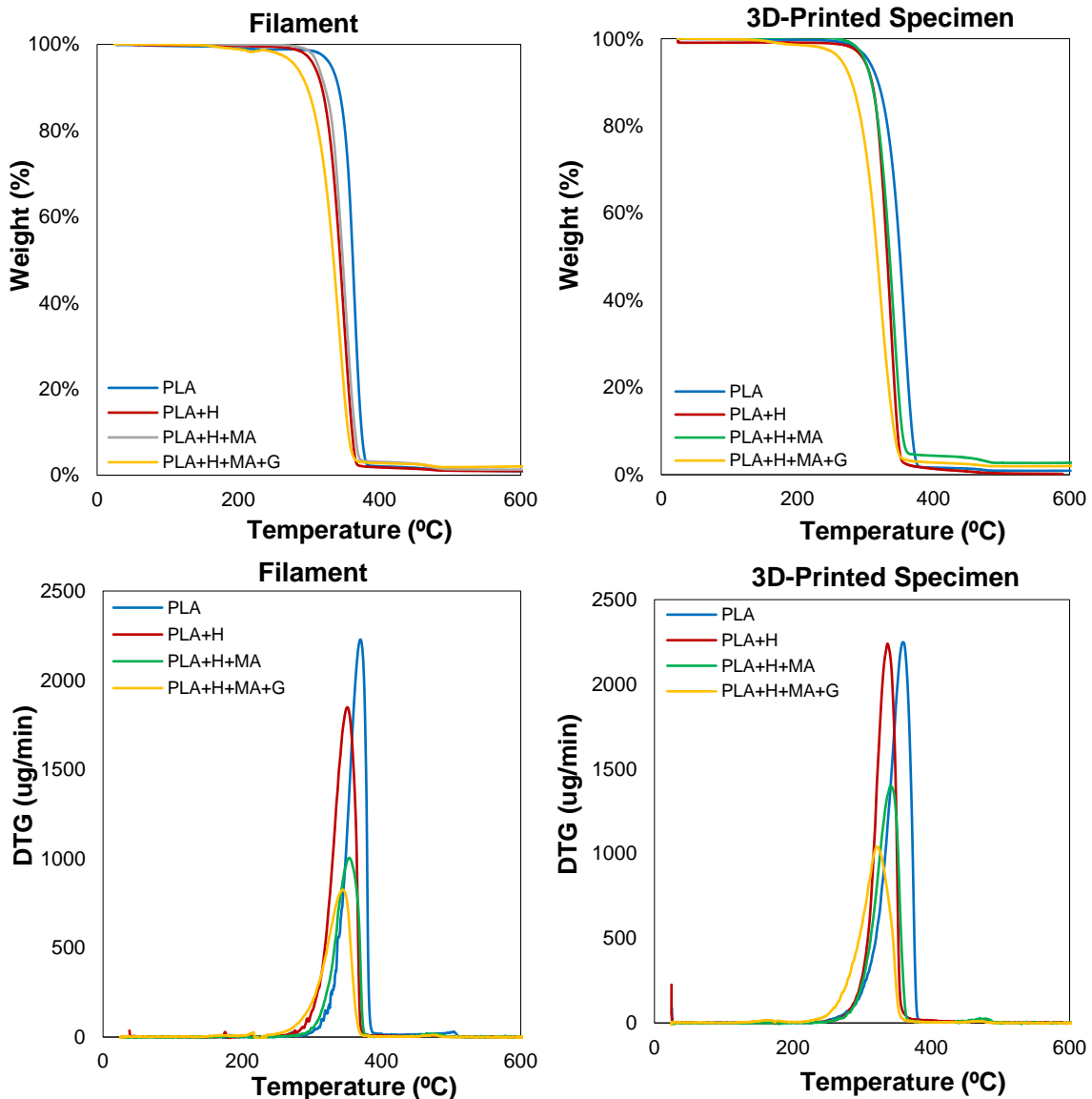


Fig. 3. TGA curves for PLA and biocomposite materials before and after 3D printing

**Table 3.** Degradation Temperatures of Biocomposite Materials (°C)

Sample Group	Filament			3D-Printed Specimen		
	$T_{5\%}$	$T_{10\%}$	$T_{90\%}$	$T_{5\%}$	$T_{10\%}$	$T_{90\%}$
PLA	331.47	341.96	374.73	303.67	318.64	368.37
PLA+H	307.47	318.25	361.18	298.25	309.65	347.18
PLA+H+MA	311.97	321.86	365.38	299.29	308.87	353.94
PLA+H+MA+G	277.48	295.84	355.55	264.01	279.59	342.14

The results obtained from the DSC analysis of the specimens of PLA and biocomposite filaments are presented in Tables 4 and 5. In Fig. 4, the blue curve represents the DSC curve from the first heating, the green curve represents the DSC curve during cooling, and the red curve represents the DSC curve from the second heating. The thermal properties of the material were examined with the first heating curve, while the second heating curve simulated for the 3D printing process how crystallinity would be changed. In the second heating curve, peaks were not observed in the sample group of biocomposite materials. Therefore, the crystallization temperature and enthalpy could not be determined. When examining the melting temperatures of the sample groups, it was observed that the values were generally close to each other. The highest melting temperature was 177.2 °C for the sample group of PLA+H+MA, while the lowest melting temperature was 172.7 °C for the sample group of PLA+H+MA+G. It was observed that the crystallinity ratio ( $X_c$ ) decreased in the PLA+H and PLA+H+MA biocomposites compared to PLA. Lv *et al.* (2016) examined that the crystallinity of PLA/wood composites decreased from 33.7% to 26.1%, 24.7%, and 17.4% with adding of 1 wt %, 2 wt% and 3 wt %, respectively. However, adding glycerol to the PLA+H+MA composite increased the crystallinity ratio by 17.7%. According to the DSC results, the PLA+H+MA+G group had the highest crystallinity ratio, similar to that of PLA. This indicated that adding glycerol to the biocomposite helps maintain the proportion of crystalline regions in the material. The group with the highest  $T_g$  was the sample group of PLA+H+MA, while those of the lowest was observed in the sample group of PLA. A higher  $T_g$  often indicates that the material is stiffer and more brittle. According to the results from the tensile test, the tensile strength value of the PLA+H+MA group was lower compared to the other sample groups. Moreover, Dogru *et al.* (2022) observed that a 10% by-weight hemp fiber addition to PLA bioplastics increased the tensile strength by 20% and raised the  $T_g$  while decreasing the melting temperature and thermal resistance. A 3% by-weight hemp fiber addition in this study resulted in only a 2.5% increase in tensile strength, and the thermal analysis results also confirmed the findings in the literature.

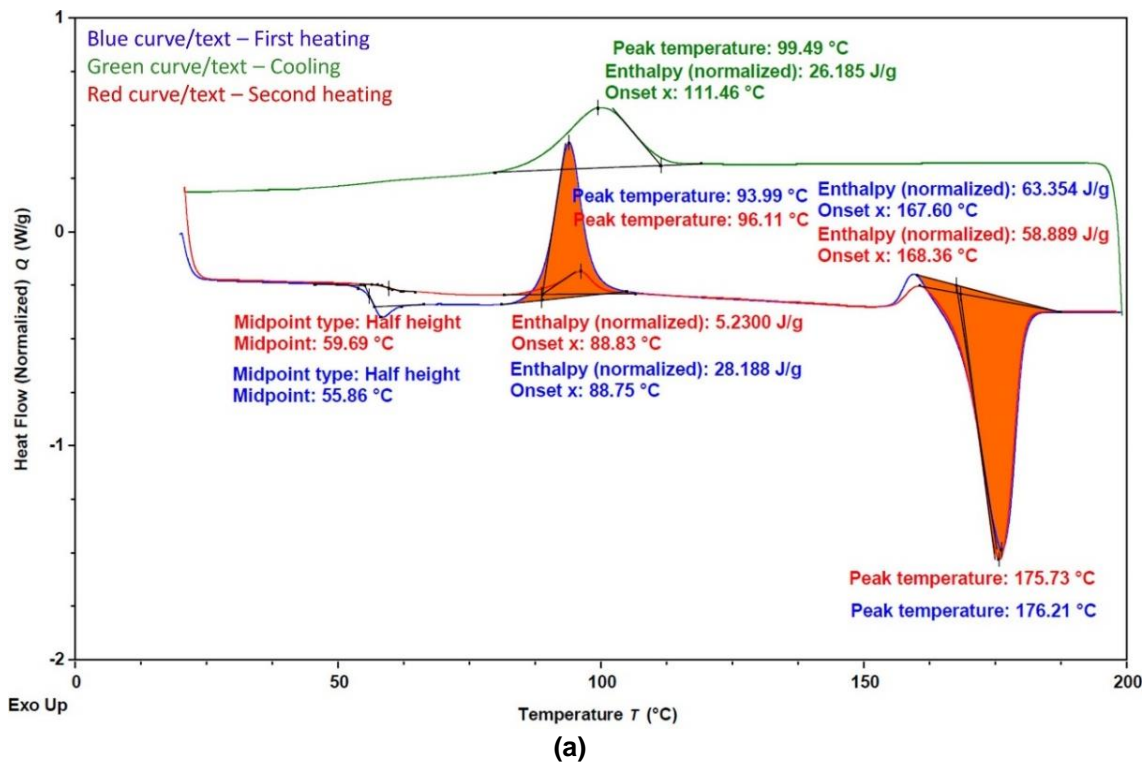
Another conclusion from the DSC results is that the crystallization enthalpy of the PLA in the cooling step is lower than those of the composites indicating noncompleted crystallization of the PLA chains. This conclusion is supported by the observed cold crystallization peak in the second heating of PLA, whereas there were no observed cold crystallization for the composites in the second heating. So, it can be said that the hemp facilitates the crystallization of the PLA. Supportively, Fortunati *et al.* (2012) reported nucleating agent effect of cellulose nanocrystals for crystallization behavior the PLA. Another observation from the results is that glycerol addition significantly decreased to cold crystallization temperature in the first heating. This is because of the plastifying effect of the glycerol. Similarly, it is reported that PEG, as a plasticizer, decreased the cold crystallization temperature of PLA (Li and Huneault 2007).

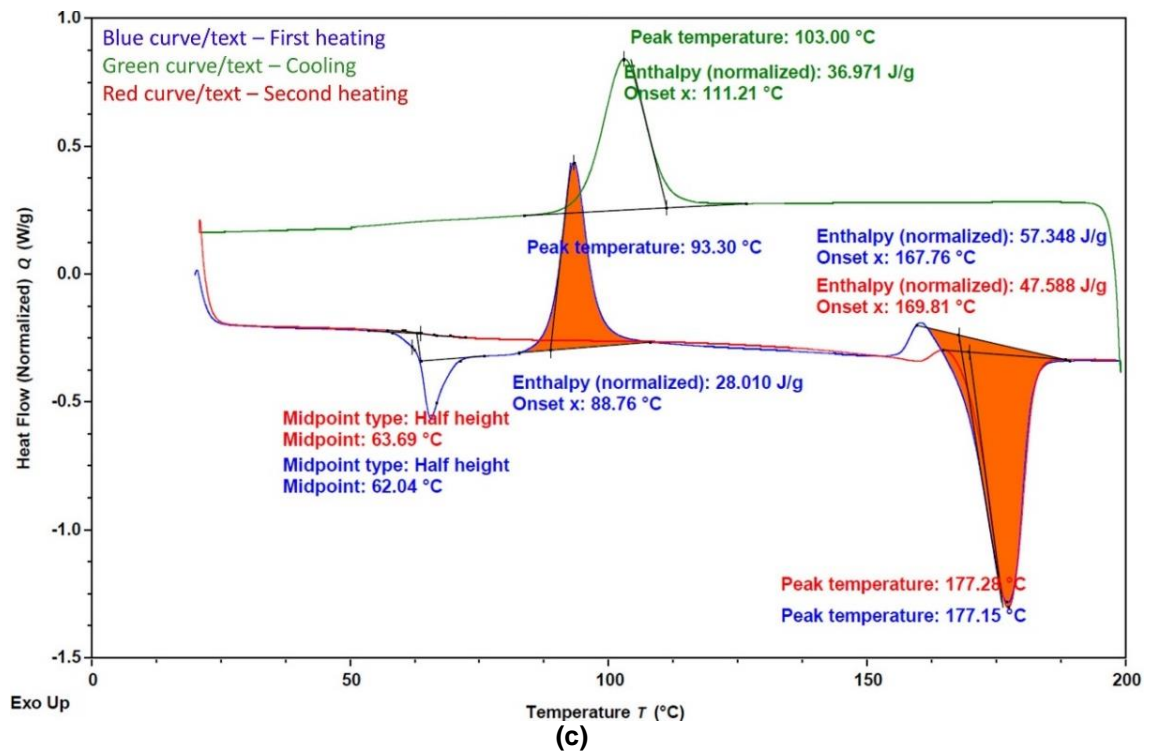
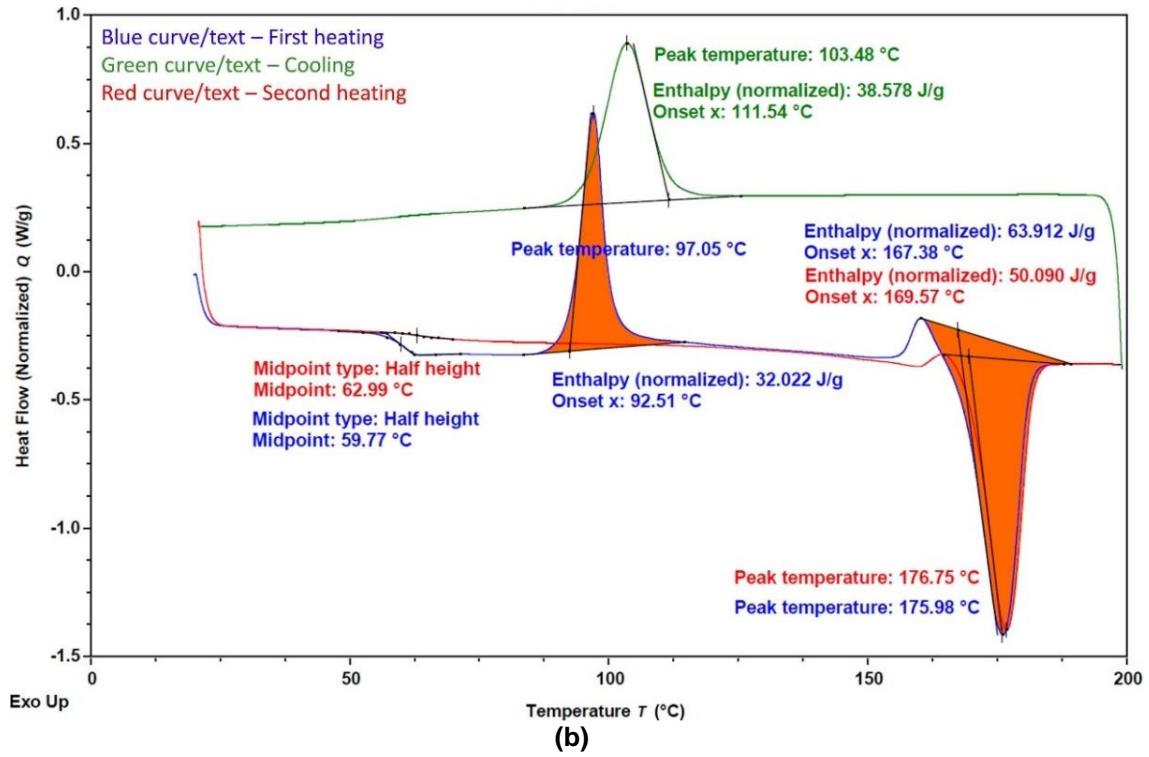
**Table 4.** DSC Results for PLA and Biocomposite Materials During the First Heating

Sample Group	$T_g$ (°C)	$T_{cc}$ (°C)	$T_m$ (°C)	$\Delta H_m$ (J/g)	$\Delta H_{cc}$ (J/g)	$X_c$ (%)
PLA	55.86	93.99	176.21	63.35	28.19	37.81
PLA+H	59.77	97.05	175.98	63.91	32.02	35.35
PLA+H+MA	62.04	93.30	177.15	57.35	28.01	32.52
PLA+H+MA+G	56.97	85.49	172.74	60.42	25.88	38.28

**Table 5.** DSC Results for PLA and Biocomposite Materials during the Second Heating

Sample Group	$T_g$ (°C)	$T_{cc}$ (°C)	$T_m$ (°C)	$\Delta H_m$ (°C)	$\Delta H_{cc}$ (°C)	$X_c$ (%)
PLA	59.69	96.11	175.21	58.88	5.23	57.70
PLA+H	62.99	-	176.75	50.09	-	55.53
PLA+H+MA	62.04	-	177.28	47.58	-	52.75
PLA+H+MA+G	56.97	-	173.61	44.88	-	49.75





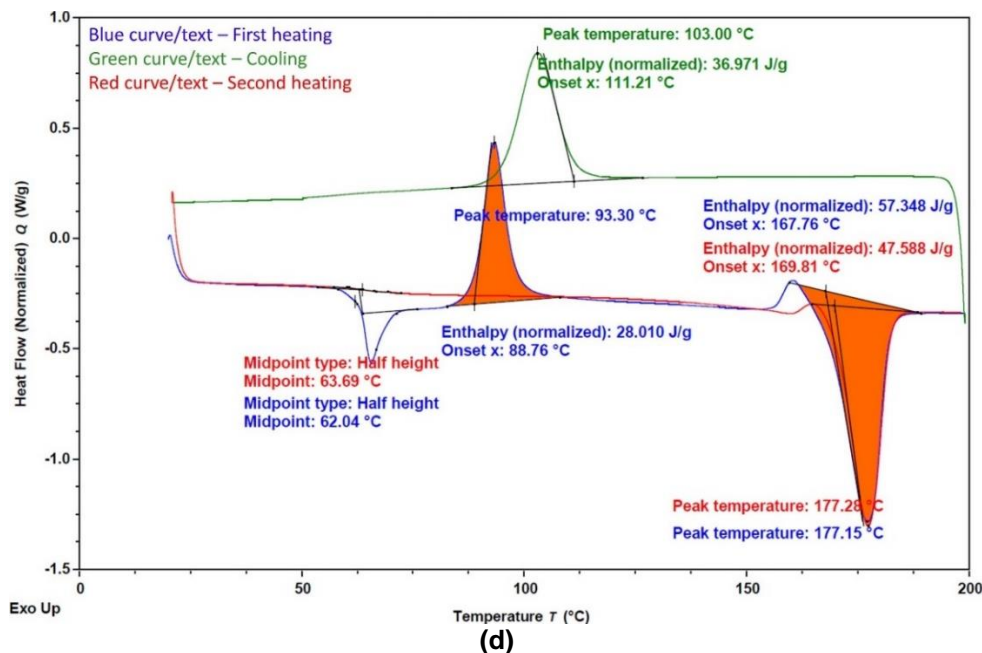


**Fig. 4.** DSC curves for (a) PLA, (b) PLA+H, (c) PLA+H+MA, and (d) PLA+H+MA+G

### FTIR Analysis of Materials

The FTIR spectrum of the components used in biocomposite materials is shown in Fig. 5a. In addition, the FTIR spectrum of PLA and biocomposite materials is presented in Fig. 5b. Adding maleic anhydride did not result in detectable interaction between the components. Maleic acid has a characteristic peak at  $1700\text{ cm}^{-1}$ . The peak intensity decreased in the sample group to which glycerol was added. This indicated that MA also interacted when glycerol was added to the biocomposite materials. In the sample group of PLA+H+MA, the addition of MA resulted in forming a broad peak in the region of  $3000$  to  $3500\text{ cm}^{-1}$ . Because maleic acid ester has a characteristic peak in this region, it can be inferred that adding MA leads to the formation of maleic acid ester under the influence of temperature.

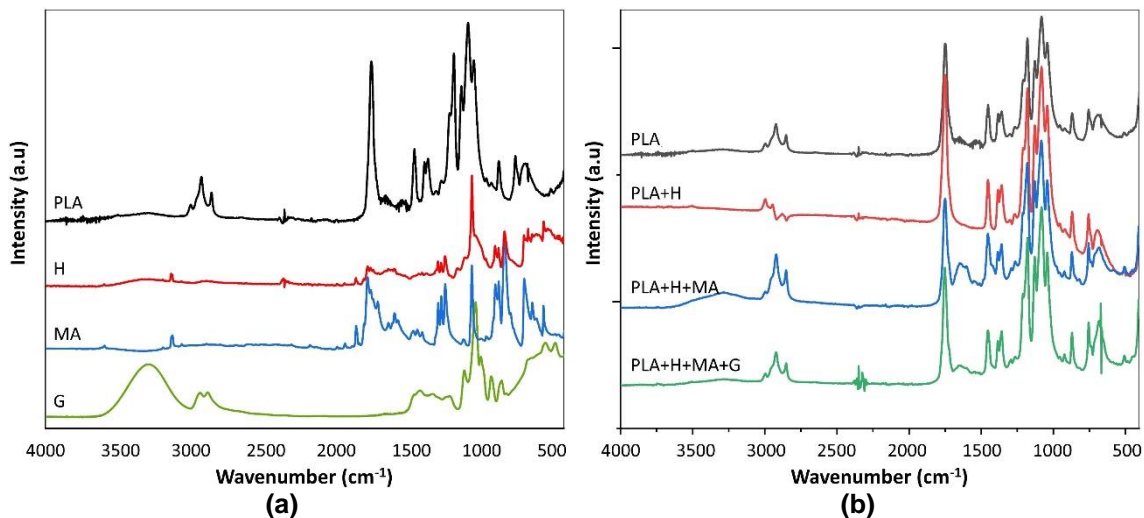


**Fig. 5.** FT-IR spectra: (a) Compounds of biocomposite, and (b) PLA and biocomposite materials

## SEM Analysis

The SEM analysis showed that adding hemp fiber to PLA bioplastic (Fig. 6b) in the study reduced the brittleness on surfaces. Adding MA (Fig. 6c) further decreased this brittleness, and including glycerol (Fig. 6d) resulted in a more ductile structure. In Fig. 6a, the fractured surface of the PLA in the tension test failed by obtaining a surface pattern as ruptured, whereas those of PLA+H+MA+G failed as a sticky pattern. The 3D printing could also be performed with the layer widths and heights, as given in Fig. 6e, using a nozzle diameter of 0.6 mm and a layer thickness of 0.3 mm. Additionally, the diameter of the hemp fiber used as a filler material in Fig. 6f was not greater than approximately 10  $\mu\text{m}$ . Still, it was not competent to measure the length of the hemp fiber on the fractured surface. A better bonding between the layers during the 3D printing stage was observed in PLA (Fig. 6g) and PLA+H (Fig. 6h) materials. However, in the PLA+H+MA biocomposite (Fig. 6i) and PLA+H+MA+G (Fig. 6j) biocomposites, it was observed that there was no complete adhesion between the layers. The lower tensile strength of these materials compared to PLA and PLA+H can be suggested as reasons for these results. In PLA+H+MA (Fig. 6k) and PLA+K03+MA+G (Fig. 6l) materials, it was observed that hemp fiber and MA additives detached from the surfaces, indicating that the materials did not form a good interface with each other in the biocomposite. This explains the low tensile strength of these materials as discussed.

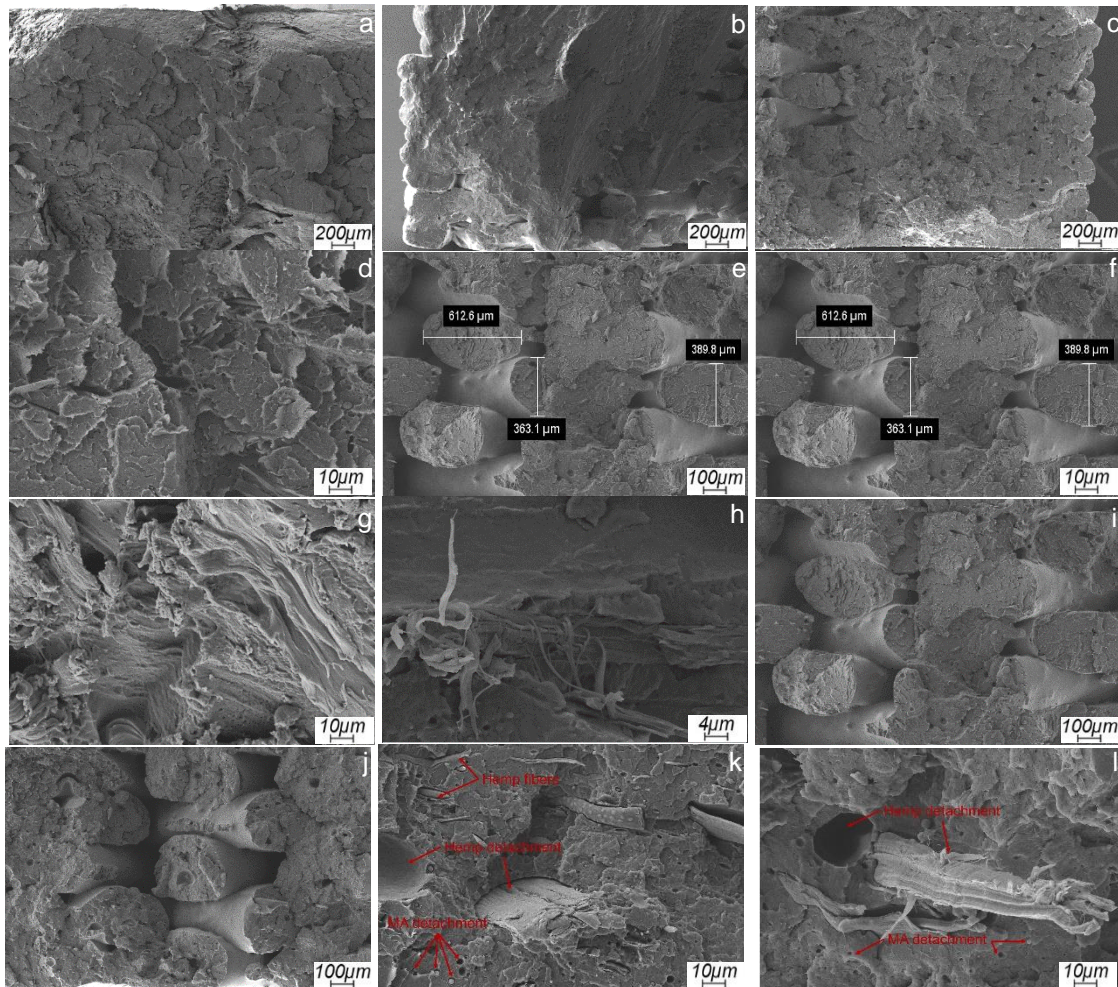


**Fig. 6.** SEM images for bioplastic and biocomposites used in the study

## Mechanical Properties of PLA and Biocomposite Materials

The test samples composed of PLA, PLA+H, PLA+H+MA, and PLA+H+MA+G were manufactured using additive methods. The impact of the changes in material composition on tensile strength (TS), MOE, and flexural strength (FS) was statistically analyzed across 20 samples divided into four different groups. Results for the FS, MOE, and TS are given in Fig. 7. According to the results, the TS of PLA was slightly increased (about 2%) by adding 3 wt% hemp fiber, but dramatically reduced 20% after adding MA. Adding glycerol to PLA+H+MA increased the TS of the biocomposite 14%. The decrease found after adding MA and G could be explained by the interface between layers during the FFF process due to decreased melt flow (Turner and Gold 2015) as shown in Fig. 6i and Fig. 6j. Moreover, in DSC analysis, the  $T_g$  for PLA+H+MA+G was lowest for both before and after 3D printing.

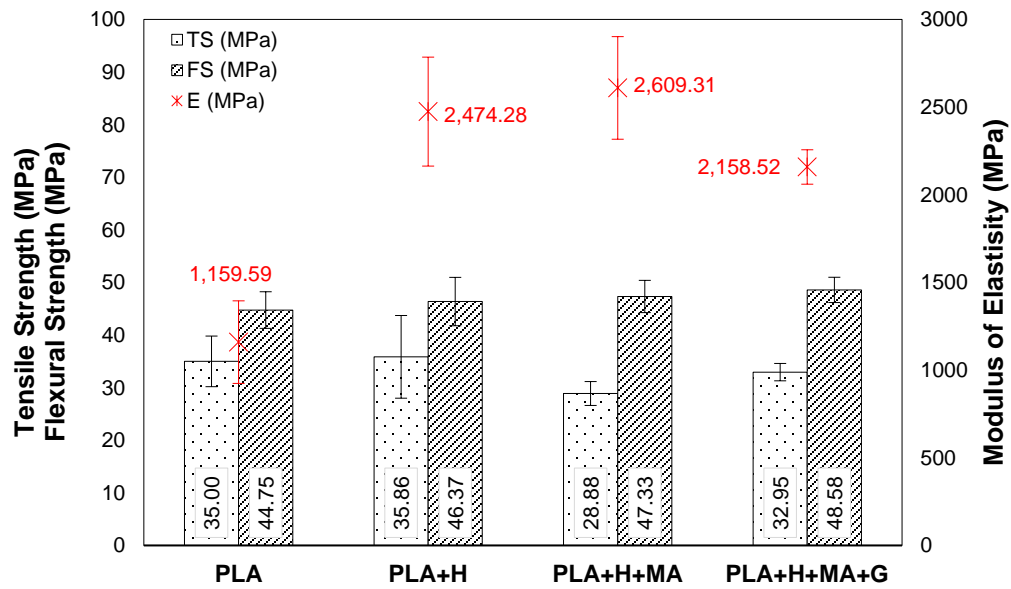


Fig. 7. Tensile strength, flexural strength, and modulus of elasticity of the materials

As shown in Table 6, the linear model constructed to examine the effect of changes in material composition on the dependent variable TS, within a 95% confidence interval (CI), yielded an R-squared value of 16.76% and an adjusted R-squared value of 1.15%. The analysis of variance conducted within the same model revealed that the material independent variable had a p-value of 0.076. This indicated that the changes in material composition do not have a statistically significant effect on the TS of the material.

Table 6. ANOVA for Tensile Strength of PLA and Biocomposite Materials

Source	DF	Adj SS	Adj MS	F-Value	P-Value
Material	3	0.00	0.00	2.77	0.076
Error	16	0.00	0.00		
Total	19	0.00			
S	R-sq	R-sq(adj)		R-sq(pred)	
1.25511	16.76%	1.15%		0.00%	

The results of the Tukey pairwise comparison, conducted at a 95% CI, for the average TS values of the samples in four different groups, are presented in Table 7. Although the PLA+H+MA group, which contains filaments with a 3% hemp fiber additive, had the highest transformed average TS value, the analysis results at a 95% CI indicated that there were no statistically significant differences in the mean TS values among the groups with different material compositions. From Fig. 8, it can also be inferred that all pairwise comparison CIs include the value “0,” indicating that the corresponding mean values were not statistically different from each other.

**Table 7.** Tukey Pairwise Comparison Results for Tensile Strength of PLA and Biocomposite Materials

Material	N	Mean	Grouping
PLA+H+MA	5	0.0000407	A
PLA+H+MA+G	5	0.0000283	A
PLA+H	5	0.0000258	A
PLA	5	0.0000256	A

\*Means that do not share a letter are significantly different

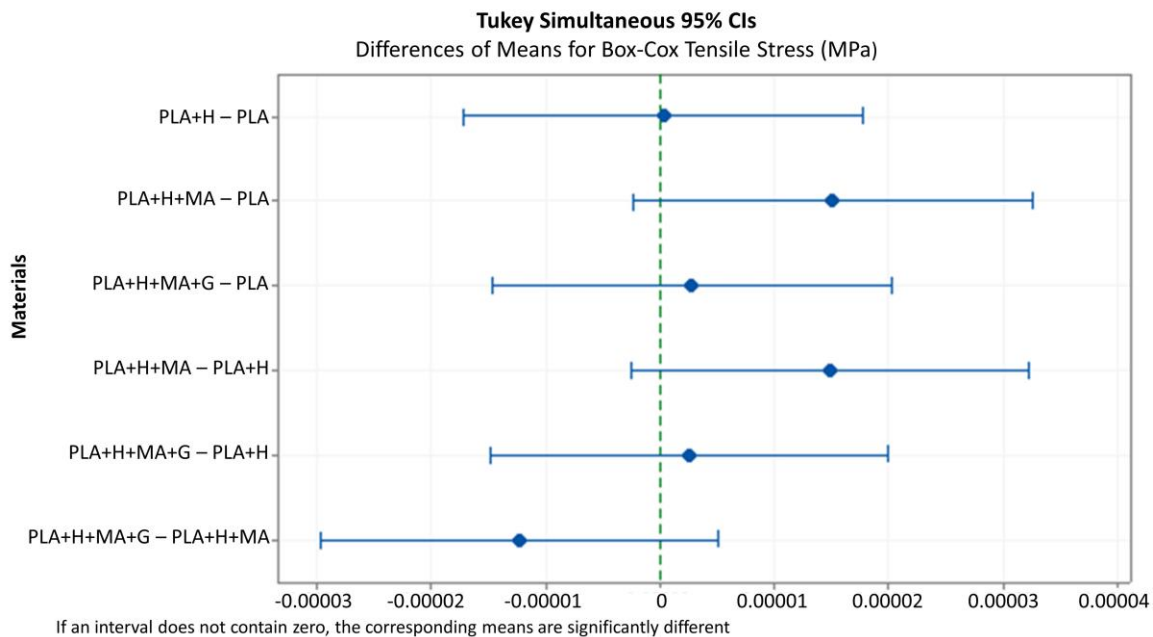


**Fig. 8.** Tukey method of pairwise comparison results for tensile strength of PLA and biocomposite materials

In flexural strength, adding ingredients of biocomposites moderately increased material strength. Neat PLA had the lowest FS (44.75 MPa). Adding hemp fiber, MA, and glycerol to composite increased FS 3.6%, 2.1%, and 2.6%, respectively. Adding hemp fiber as a stress raiser contributed to purportedly increased yielding (Xiao *et al.* 2019); correspondingly, brittleness of the 3D-printed specimens in FFF was also increased. In addition, adding MA to biocomposites increased the flexural strength (Lv *et al.* 2016). The results of the ANOVA conducted to examine the effect of the material composition on the dependent variable FS are presented in Table 8. The developed linear model had an R-squared value of 16.8% and an adjusted R-squared value of 1.15%, indicating that the

model had a weak ability to explain the variance in the FS values. As can be seen in Table 8, this inferential observation was supported by the high p-value of 0.388 for the material independent variable within the 95% CI.

**Table 8.** ANOVA for Effects of Ingredients on Flexural Strength of PLA and Biocomposite Materials

Source	DF	Adj SS	Adj MS	F-Value	P-Value
Material	3	5.075	1.692	1.07	0.388
Error	16	25.205	1.575		
Total	19	30.280			
S	R-sq	R-sq(adj)		R-sq(pred)	
1.25511	16.76%	1.15%		0.00%	

The Tukey pairwise comparison results, conducted to observe the statistical differences in the average FS values of the samples in four different groups, were consistent with the ANOVA analysis results. The PLA+H+MA+G group, with an average log and Box-Cox transformed FS value of 13.6 MPa had the mean value, while the control group had a mean FS value of 12.3 MPa. As shown in Table 9, the transformed mean FS values for all material composition groups fell within a single class at the 95% CI, indicating no statistically significant differences.

**Table 9.** Tukey Pairwise Comparison Results for Flexural Strength of PLA and Biocomposite Materials

Material	N	Mean	Grouping
PLA+H+MA+G	5	13.64	A
PLA+H+MA	5	13.19	A
PLA+H	5	12.84	A
PLA	5	12.26	A

\*Means that do not share a letter are significantly different.

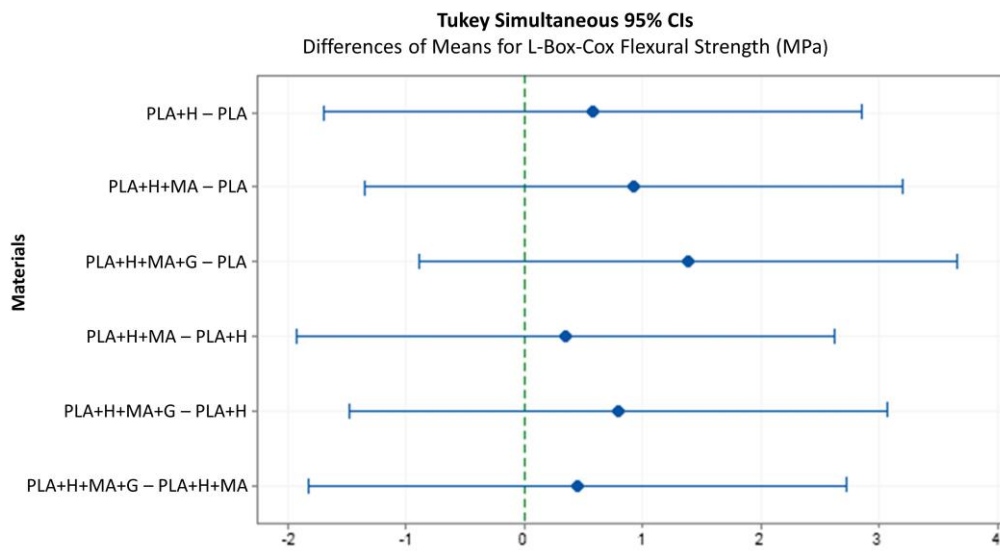


**Fig. 9.** Tukey method of pairwise comparison results for flexural strength of PLA and biocomposite materials

From Fig. 9, it can also be inferred that all pairwise comparison confidence intervals include the value "0," indicating that the corresponding mean values were not statistically different from each other.

The potential changes in the MOE when the production recipe for filament includes hemp fiber, maleic anhydride, and glycerol were statistically examined. As shown in Table 10, the material independent variable was found to have a statistically significant effect on the dependent variable MOE, with a p-value of less than 0.0001 within a 95% CI. The linear model constructed as part of the analysis had an R-squared value of 76.80% and an adjusted R-squared value of 72.45%. These values indicated the presence of a strong linear relationship, suggesting that the material composition could explain 72.45% of the observed variance in MOE values.

**Table 10.** ANOVA for Effects of Ingredients on MOE of PLA and Biocomposite Materials

Source	DF	Adj SS	Adj MS	F-Value	P-Value
Material	3	3273001	1091002	17.65	< 0.0001
Error	16	988861	61804		
Total	19	4261868			
S	R-sq	R-sq(adj)		R-sq(pred)	
248.604	76.80%	72.45%		63.75%	

Tukey pairwise comparison results were analyzed to further investigate the impact of changes in the material recipe on the average MOE. According to these results, the average MOE value of the group containing only PLA samples (1560 MPa), was found to be statistically different from the average MOE values of the PLA+H, PLA+H+MA, and PLA+H+MA+G groups at a 95% CI. These findings are presented in Table 11 and Fig. 10. The pairwise comparison results between the PLA+H and PLA+H+MA groups and between the PLA+H and PLA+H+MA+G groups did not show statistically significant differences within the 95% CI. However, the pairwise comparison results between the PLA+H+MA and PLA+H+MA+G groups indicated that the average MOE values of these groups were statistically different.

**Table 11.** Tukey Pairwise Comparison Results for MOE of PLA and Biocomposite Materials

Material	N	Mean	Grouping		
PLA+H+MA	5	2609.31	A		
PLA+H	5	2474.28	A	B	
PLA+H+MA+G	5	2158.52		B	
PLA	5	1559.59			C

\*Means that do not share a letter are significantly different

Because the models developed for the dependent variables of TS and FS did not show statistically significant effects, the Main Effects Plot was created solely for the MOE variable and is presented in Fig. 11. As depicted, the addition of 3% hemp fiber to the material composition significantly increased the average elastic modulus. The inclusion of MA addition to hemp fiber resulted in a higher mean value yet showed a weaker positive effect on the elastic modulus when compared to the change between mean values of PLA and PLA+H groups. In contrast, the addition of glycerol negatively impacted the mean

elasticity value. After adding MA, the mean elasticity value rose to 2610 MPa but then declined to 2160 MPa with the addition of glycerol.

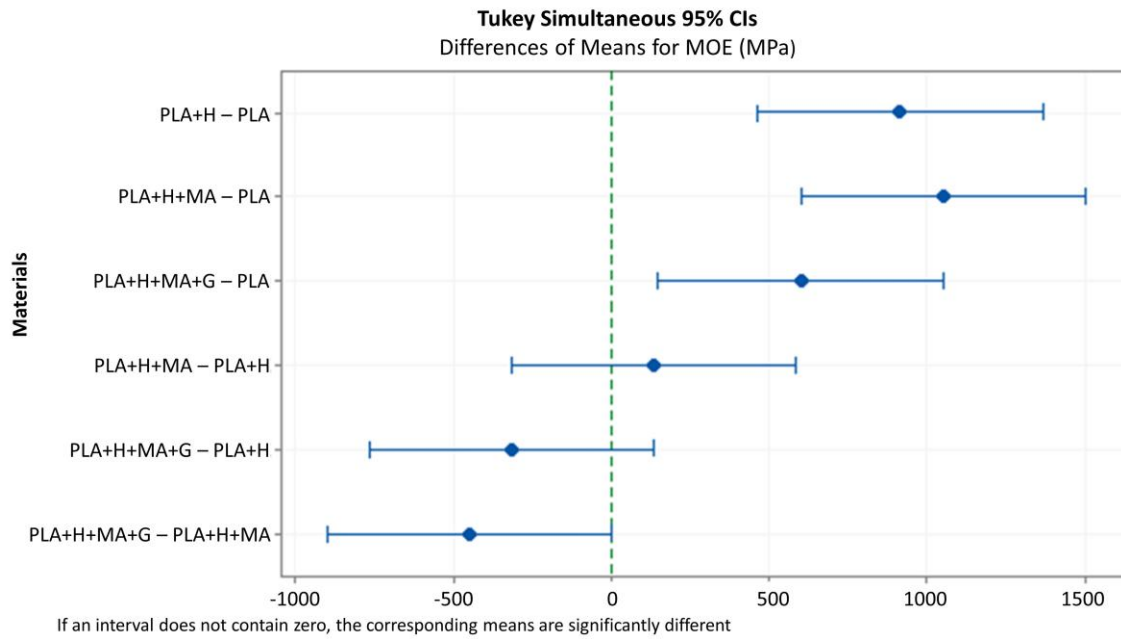


**Fig. 10.** Tukey method of pairwise comparison results for MOE of PLA and biocomposite materials

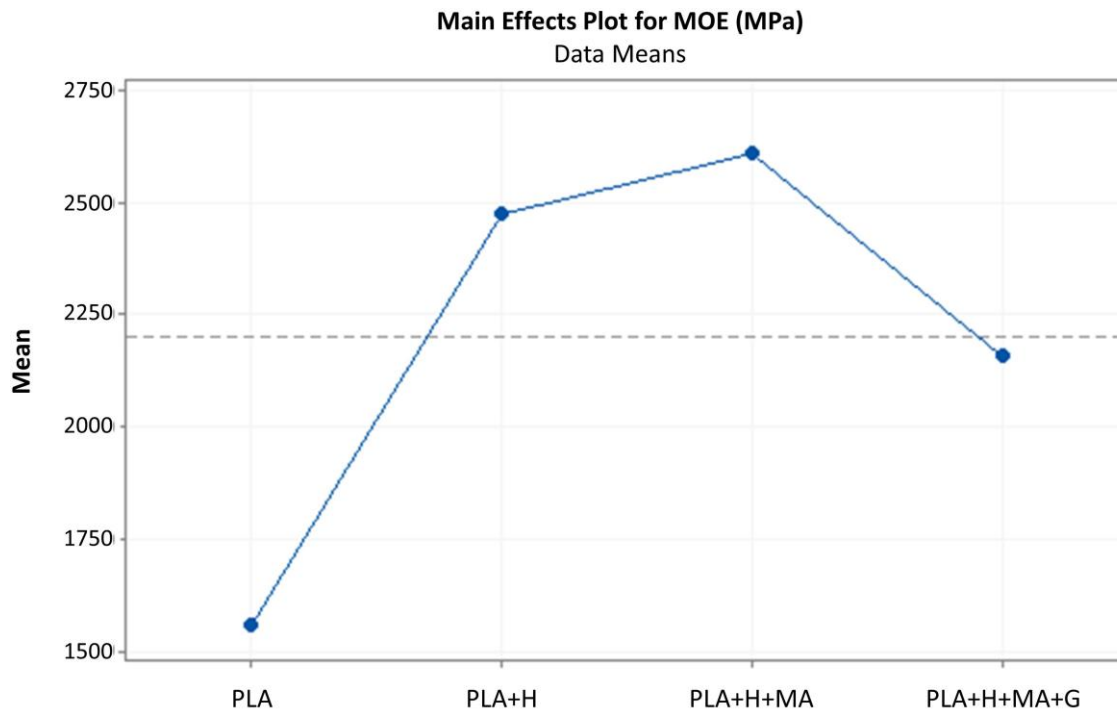


**Fig. 11.** Main effects plot for MOE of PLA and biocomposite materials

## CONCLUSIONS

This study produced eco-friendly biocomposite filaments for 3D printing. The tensile and flexural test specimens were successfully printed using the specified layer width and height values. This study monitored the changes that occurred in the mechanical, thermal, and morphological properties of the biocomposite materials prepared by adding hemp fiber, maleic anhydride, and glycerol to poly(lactic acid) (PLA) bioplastics.

1. The Fourier transform infrared (FTIR) analysis revealed that the highest interaction between the materials occurred in the PLA+H+MA+G group, where H is hemp, MA is maleic anhydride, and G is glycerol. This group also exhibited the highest degree of crystallinity and flexural strength. The scanning electron microscopy (SEM) images supported these results by showing that this group had a more ductile structure. The PLA+H+MA+G biocomposite had the lowest thermal stability and melting temperature among the experimental groups.
2. The PLA+H+MA group had the lowest degree of crystallinity and the highest glass transition temperature and melting temperature. It also had the highest flexural modulus of elasticity. Adding 3% hemp fiber and maleic anhydride to PLA increased the modulus of elasticity (MOE) by approximately 125%. Although the groups had no statistically significant difference in tensile strength (TS) values, the PLA+H+MA group had the lowest TS.
3. The addition of only 3% hemp fiber to PLA maintained tensile properties, with the highest TS observed in the PLA and PLA+H groups. The neat PLA group had the lowest glass transition temperature and the highest thermal stability. According to the bending test results, the lowest flexural strength (FS) was observed in PLA. Adding hemp fiber and other materials to the structure improved the bending strength in mathematical terms, although statistically, the flexural properties of PLA were preserved. The flexural MOE significantly increased with addition of hemp fiber to the PLA structure.
4. The SEM analysis showed that adding hemp fiber to the PLA matrix reduced the brittleness of the PLA material, and the glycerol addition contributed to a more ductile structure. Adding hemp to the PLA matrix formed an excellent interface between layers. At the same time, the MA addition hindered the formation of a good interface between hemp fiber and PLA, leading to fiber pull-out during failure. Although treating hemp fibers with MA was intended to improve the interface between hemp fiber and PLA, the expected results were not achieved. This may be due to the amount of MA used. Further studies should explore different concentrations of MA and alternative treatment methods for more objective results.

Future work should focus on producing materials with higher hemp fiber content by using crosslinking agent such as dicumyl peroxide (DCP) and different compatibilizers and considering the impact of 3D printing parameters on the mechanical properties of the produced parts, as noted in the literature. Therefore, using different printing parameters is also vital. In the next phase, conducting final product trials with the produced material will be crucial for commercializing the product.

## ACKNOWLEDGMENTS

This manuscript was a part of the M.S. thesis entitled “Investigation of some mechanical and thermal properties of hemp/PLA biocomposite material manufactured by fused deposition modeling” in the Department of Biocomposite Engineering at Bursa Technical University.

## REFERENCES CITED

- Ali, S., Nouzil, I., Mehra, V., Eltaggaz, A., Deiab, I., and Pervaiz, S. (2024). “Integrated optimization scheme for 3D printing of PLA-APHA biodegradable blends,” *Progress in Additive Manufacturing 2024*, available online. DOI:10.1007/s40964-024-00684-z
- Almeida, V. H. M., Jesus, R. M., Santana, G. M., and Pereira, T. B. (2024). “Polylactic acid polymer matrix (PLA) biocomposites with plant fibers for manufacturing 3D printing filaments: A review,” *Journal of Composites Science* 8(2), article ID 67. DOI: 10.3390/jcs8020067
- Ambade, V. V., Padole, V., and Badole, B. (2023). “Effect of infill density, infill pattern and extrusion temperature on mechanical properties of part produced by 3D printing FDM technology using ABS, PLA and PETG filament: A critical review,” *International Journal of Research and Analytical Reviews* 10(1), 130-136.
- Antony, S., Cherouat, A., and Montay, G. (2020). “Fabrication and characterization of hemp fibre based 3D printed honeycomb sandwich structure by FDM process,” *Applied Composite Materials* 27(6), 935-953. DOI: 10.1007/s10443-020-09837-z
- Arnold, J., and Smith, D. A. (2021). “3D printed polylactic acid - hemp fiber composites: Mechanical, thermal, and microcomputed tomography data,” *Data in Brief* 39, article ID 107534. DOI: 10.1016/j.dib.2021.107534
- Arumaiselvan, U., Kalimuthu, M., Nagarajan, R., Mohan, M., Ismail, S.O., Mohammed, F., Al-Lohedan, H.A., and Krishnan, K. (2024). “Mechanical, physical and thermal properties of polylactic acid filament composite reinforced with newly isolated *Cryptostegia grandiflora* fiber,” *BioResources* 19(2), 3740-3754. DOI: 10.15376/biores.19.2.3740-3754
- Arockiam, A. J., Subramanian, K., Padmanabhan, R. G., Selvaraj, R., Bagal, D. K., and Rajesh, S. (2021). “A review on PLA with different fillers used as a filament in 3D printing,” *Materials Today: Proceedings* 50, 2057-2064. DOI: 10.1016/j.matpr.2021.09.413
- ASTM D638 (2010). “Standard test for tensile properties of plastics,” ASTM International, West Conshohocken, PA, USA.
- ASTM D790 (2010). “Standard test methods for flexural properties of unreinforced and reinforced plastics and electrical insulating materials,” ASTM International, West Conshohocken, PA, USA.
- ASTM F2792 (2012). “Standard terminology for additive manufacturing technologies,” ASTM International, West Conshohocken, PA, USA.
- Baghaei, B., Skrifvars, M., Salehi, M., Bashir, T., Rissanen, M., and Nousiainen, P. (2014). “Novel aligned hemp fibre reinforcement for structural biocomposites: Porosity, water absorption, mechanical performances and viscoelastic behaviour,” *Composites Part A: Applied Science and Manufacturing* 61, 1-12. DOI: 10.1016/j.compositesa.2014.01.017

- Bianchi, I., Forcellese, A., Gentili, S., Greco, L., and Simoncini, M. (2022). "Comparison between the mechanical properties and environmental impacts of 3D printed synthetic and bio-based composites," *Procedia CIRP* 105, 380-385. DOI: 10.1016/j.procir.2022.02.063
- Bragaglia, M., Cecchini, F., Paleari, L., Ferrara, M., Rinaldi, M., and Nanni, F. (2023). "Modeling the fracture behavior of 3D-printed PLA as a laminate composite: Influence of printing parameters on failure and mechanical properties," *Composite Structures* 322, article ID 117379. DOI: 10.1016/j.compstruct.2023.117379
- BS EN ISO 11357-3 (2021). "Plastics — Differential scanning calorimetry (DSC) Part 3: Determination of temperature and enthalpy of melting and crystallization," British Standard Institute, London, UK.
- BS EN ISO 11357-4 (2021). "Plastics — Differential scanning calorimetry (DSC) Part 4: Determination of specific heat capacity," British Standard Institute, London, UK.
- BS EN ISO 11358-1 (2014). "Plastics. Thermogravimetry (TG) of polymers General principles," British Standard Institute, London, UK.
- Calì, M., Pascoletti, G., Gaeta, M., Milazzo, G., and Ambu, R. (2020). "New filaments with natural fillers for FDM 3D printing and their applications in biomedical field," *Procedia Manufacturing* 51(2019), 698-703. DOI: 10.1016/j.promfg.2020.10.098
- DeStefano, V., Khan, S., and Tabada, A. (2020). "Applications of PLA in modern medicine," *Engineered Regeneration* 1, 76-87. DOI: 10.1016/j.engreg.2020.08.002
- Dogru, A., Sozen, A., Nesar, G., and Seydibeyoglu, M. O. (2021). "Effects of aging and infill pattern on mechanical properties of hemp reinforced PLA composite produced by fused filament fabrication (FFF)," *Applied Science and Engineering Progress* 14(4), 651-660. DOI: 10.14416/j.asep.2021.08.007
- Doğru, A., Sözen, A., Seydibeyoğlu, M. Ö., and Neşer, G. (2022). "Hemp reinforced polylactic acid (PLA) composite produced by fused filament fabrication (FFF)," *Hacettepe Journal of Biology and Chemistry* 50(3), 239-246.
- Edyta, M., Piotr, P., Marcin, D., and Kamila, B. (2015). "Comparison of papermaking potential of wood and hemp cellulose pulps," *Forestry and Wood Technology* 91, 134-137.
- Fike, J. (2016). "Industrial hemp: Renewed opportunities for an ancient crop," *Critical Reviews in Plant Sciences* 35(5–6), 406-424. DOI: 10.1080/07352689.2016.1257842
- Fortunati, E., Armentano, I., Zhou, Q., Puglia, D., Terenzi, A., Berglund, L. A., and Kenny, J. M. (2012). "Microstructure and nonisothermal cold crystallization of PLA composites based on silver nanoparticles and nanocrystalline cellulose," *Polymer Degradation and Stability* 97(10), 2027-2036. DOI: 10.1016/j.polymdegradstab.2012.03.027
- Getme, A. S., and Patel, B. (2019). "A review: Bio-fibers as reinforcement in composites of polylactic acid (PLA)," *Materials Today: Proceedings* 26, 2116-2122. DOI: 10.1016/j.matpr.2020.02.457
- Guessasma, S., Nouri, H., and Belhabib, S. (2022). "Digital image correlation to reveal mechanical anisotropy in 3D printing of polymers," *Materials* 15, article 8382. DOI: 10.1080/14786435.2022.2140217
- Halloran, M. W., Danielczak, L., Nicell, J. A., Leask, R. L., and Marić, M. (2022). "Highly flexible polylactide food packaging plasticized with nontoxic, biosourced glycerol plasticizers," *ACS Applied Polymer Materials* 4(5), 3608-3617. DOI: 10.1021/acsapm.2c00172

- Ilyas, R. A., Sapuan, S. M., Harussani, M. M., Hakimi, M. Y. A. Y., Haziq, M. Z. M., Atikah, M. S. N., Asyraf, M. R. M., Ishak, M. R., Razman, M. R., Nurazzi, N. M., *et al.* (2021). "Polylactic acid (PLA) biocomposite: Processing, additive, manufacturing and advanced applications," *Polymers* 13, article ID 1326. DOI: 10.3390/polym13081326
- Jałbrzykowski, M., Oksiuta, Z., Obidziński, S., Czyżewska, U., Osiecki, T., Kroll, L., and Joka Yildiz, M. (2022). "Assessment of innovative PLA biopolymer compositions with plant waste fillers," *Engineering Failure Analysis* 139, article ID 106496. DOI: 10.1016/j.engfailanal.2022.106496
- Jiang, Z., Diggle, B., Tan, M. L., Viktorova, J., Bennett, C. W., and Connal, L. A. (2020). "Extrusion 3D printing of polymeric materials with advanced properties," *Advanced Science* 7, article ID 2001379. DOI: 10.1002/advs.202001379
- Kajbič, J., Fajdiga, G., and Klemenc, J. (2023). "Material extrusion 3D printing of biodegradable composites reinforced with continuous flax fibers," *Journal of Materials Research and Technology* 27, 3610-3620. DOI: 10.1016/j.jmrt.2023.10.148
- Kananathan, J., Samykano, M., Kadirgama, K., Ramasamy, D., and Rahman, M. M. (2022). "Comprehensive investigation and prediction model for mechanical properties of coconut wood–polylactic acid composites filaments for FDM 3D printing," *European Journal of Wood and Wood Products* 80(1), 75-100. DOI: 10.1007/s00107-021-01768-1
- Khan, S. A., Khan, S. B., Khan, L. U., Farooq, A., Akhtar, K., and Asiri, A. M. (2018). "Fourier transform infrared spectroscopy: Fundamentals and application in functional groups and nanomaterials characterization," in: *Handbook of Materials Characterization*, Springer International Publishing, Cham, Switzerland, pp. 317-344. DOI: 10.1007/978-3-319-92955-2\_9
- Lares Carrillo, L. E., Salazar, J. F., Hitter, M. M., Luna, V. C., Alvarez, D. E., Arana Contreras, M., Contreras Guerrero, V. G., Hitter, J. S., Morales, D. A., Nunez, A., *et al.* (2023). "The effect of raster pattern and acetic acid exposure on the mechanical and failure properties of additively manufactured PLA and PLA-wood composite specimens," *Journal of Failure Analysis and Prevention* 23(3), 1298-1312. DOI: 10.1007/s11668-023-01681-0
- Le Duigou, A., Barbé, A., Guillou, E., and Castro, M. (2019). "3D printing of continuous flax fibre reinforced biocomposites for structural applications," *Materials & Design* 180, article ID 107884 . DOI: 10.1016/j.matdes.2019.107884
- Li, H. and Huneault, M. A. (2007). "Effect of nucleation and plasticization on the crystallization of poly (lactic acid)," *Polymer* 48(23), 6855-6866. DOI: 10.1016/j.polymer.2007.09.020
- Li, Y., Chen, M. D., Wan, X., Zhang, L., Wang, X., and Xiao, H. (2017). "Solvent-free synthesis of the cellulose-based hybrid beads for adsorption of lead ions in aqueous solutions," *RSC Advances* 7(85), 53899-53906. DOI: 10.1039/C7RA09592A
- Luedtke, J., Gaugler, M., Grigsby, W. J., and Krause, A. (2019). "Understanding the development of interfacial bonding within PLA/wood-based thermoplastic sandwich composites," *Industrial Crops and Products* 127, 129-134. DOI: 10.1016/j.indcrop.2018.10.069
- Lv, S., Gu, J., Tan, H., and Zhang, Y. (2016). "Modification of wood flour/PLA composites by reactive extrusion with maleic anhydride," *Journal of Applied Polymer Science* 133(15), article 43295. DOI: 10.1002/app.43295

- Mantelli, A., Romani, A., Suriano, R., Levi, M., and Turri, S. (2022). "Additive manufacturing of recycled composites," in: *Systemic Circular Economy Solutions for Fiber Reinforced Composites, Digital Innovations in Architecture, Engineering and Construction*, Springer International Publishing, Cham, Switzerland, pp. 141-166. DOI: 10.1007/978-3-031-22352-5\_8
- Martinovic, S., Bego, M., Kukavicic, I. L., Obucina, M., and Hajdarevic, S. (2024). "Physical and mechanical properties of a new bio-composite material based on seashells for use in furniture making," *Journal of Ecological Engineering* 25(3), 1-11. DOI: 10.12911/22998993/176146
- Mazur, K. E., Borucka, A., Kaczor, P., Gądek, S., Bogucki, R., Mirzewiński, D., and Kuciel, S. (2022). "Mechanical, thermal and microstructural characteristic of 3D printed polylactide composites with natural fibers: Wood, bamboo and cork," *Journal of Polymers and the Environment* 30(6), 2341-2354. DOI: 10.1007/s10924-021-02356-3
- Mehrpouya, M., Vahabi, H., Janbaz, S., Darafsheh, A., Mazur, T. R., and Ramakrishna, S. (2021). "4D printing of shape memory polylactic acid (PLA)," *Polymer* 230, article ID 124080. DOI: 10.1016/j.polymer.2021.124080
- Mishra, A., Kumar, R., Sharma, A. K., Gupta, N. K., and Somani, N. (2024). "A statistical analysis on effect of process parameters on tensile, flexural, and hardness characteristics of wood–polylactic acid composites using FDM 3D printing," *International Journal on Interactive Design and Manufacturing* 18(3), 1303-1315. DOI: 10.1007/s12008-023-01658-1
- Mukherjee, T., and Kao, N. (2011). "PLA based biopolymer reinforced with natural fibre: A review," *Journal of Polymers and the Environment* 19(3), 714-725. DOI: 10.1007/s10924-011-0320-6
- Muthe, L. P., Pickering, K., and Gauss, C. (2022). "A review of 3D/4D printing of polylactic acid composites with bio-derived reinforcements," *Composites Part C* 8, article ID 100271. DOI: 10.1016/j.jcomc.2022.100271
- Naithani, V., Tyagi, P., Jameel, H., Lucia, L. A., and Pal, L. (2020). "Ecofriendly and innovative processing of hemp hurds fibers for tissue and towel paper," *BioResources* 15(1), 706-720. DOI: 10.15376/biores.15.1.706-720
- Paulo, A., Santos, J., da Rocha, J., Lima, R., and Ribeiro, J. (2023). "Mechanical properties of PLA specimens obtained by additive manufacturing process reinforced with flax fibers," *Journal of Composites Science* 7, article ID 27. DOI: 10.3390/jcs7010027
- Shahrubudin, N., Lee, T. C., and Ramlan, R. (2019). "An overview on 3D printing technology: Technological, materials, and applications," *Procedia Manufacturing* 35, 1286-1296. DOI: 10.1016/j.promfg.2019.06.089
- Sodergard, A., and Stolt, M. (2002). "Properties of lactic acid based polymers and their correlation with composition," *Progress in Polymer Science* 27, 1123-1163.
- Sultana, J., Rahman, M. M., Wang, Y., Ahmed, A., and Xiaohu, C. (2024). "Influences of 3D printing parameters on the mechanical properties of wood PLA filament: An experimental analysis by Taguchi method," *Progress in Additive Manufacturing* 9, 1239-1251. DOI: 10.1007/s40964-023-00516-6
- Takagi, H., Kako, S., Kusano, K., and Ousaka, A. (2007). "Thermal conductivity of PLA-bamboo fiber composites," *Advanced Composite Materials* 16(4), 377-384. DOI: 10.1163/156855107782325186

- Tarique, J., Sapuan, S. M., and Khalina, A. (2021). "Effect of glycerol plasticizer loading on the physical, mechanical, thermal, and barrier properties of arrowroot (*Maranta arundinacea*) starch biopolymers," *Scientific Reports* 11, article 13900. DOI: 10.1038/s41598-021-93094-y
- Turner, B. N., and Gold, S. A. (2015). "A review of melt extrusion additive manufacturing processes: II. Materials, dimensional accuracy, and surface roughness," *Rapid Prototyping Journal* 21(3), 250-261. DOI: 10.1108/RPJ-02-2013-0017
- Wang, H., Fu, Z., Liu, Y., Cheng, P., Wang, K., and Peng, Y. (2024). "Exploring anisotropic mechanical characteristics in 3D-printed polymer biocomposites filled with waste vegetal fibers," *Symmetry* 16, article ID 70. DOI: 10.3390/sym16010070
- Wickramasinghe, S., Do, T., and Tran, P. (2020). "FDM-based 3D printing of polymer and associated composite: A review on mechanical properties, defects and treatments," *Polymers* 12, article ID 1529. DOI: 10.3390/polym12071529
- Xiao, X., Chevali, V. S., Song, P., He, D., and Wang, H. (2019). "Polylactide/hemp hurd biocomposites as sustainable 3D printing feedstock," *Composites Science and Technology* 184, article ID 107887. DOI: 10.1016/j.compscitech.2019.107887
- Xie, G., Zhang, Y., and Lin, W. (2017). "Plasticizer combinations and performance of wood flour-poly(lactic acid) 3D printing filaments," *BioResources* 12(3), 6736-6748. DOI: 10.15376/biores.12.3.6736-6748
- Yang, T. C., and Yeh, C. H. (2020). "Morphology and mechanical properties of 3D printed wood fiber/polylactic acid composite parts using," *Polymers* 12 (6), article ID 1334. DOI: 10.3390/polym12061334
- Yang, Z., Feng, X., Xu, M., and Rodrigue, D. (2021). "Printability and properties of 3D-printed poplar fiber/polylactic acid biocomposite," *BioResources* 16(2), 2774-2788. DOI: 10.15376/biores.16.2.2774-2788
- Yu, W., Dong, L., Lei, W., Zhou, Y., Pu, Y., and Zhang, X. (2021). "Effects of rice straw powder (RSP) size and pretreatment on properties of FDM 3D-printed rsp/poly(lactic acid) biocomposites," *Molecules* 26, article ID 3234. DOI: 10.3390/molecules26113234
- Zhou, L., He, H., Li, M. C., Huang, S., Mei, C., and Wu, Q. (2018). "Enhancing mechanical properties of poly (lactic acid) through its in-situ crosslinking with maleic anhydride-modified cellulose nanocrystals from cottonseed hulls," *Industrial Crops and Products* 112, 449-459. DOI: 10.1016/j.indcrop.2017.12.044
- Zhou, L., Ke, K., Yang, M. B., and Yang, W. (2021). "Recent progress on chemical modification of cellulose for high mechanical-performance poly(lactic acid)/cellulose composite: A review," *Composites Communications* 23, article ID 100548. DOI: 10.1016/j.coco.2020.100548
- Zindani, D., and Kumar, K. (2019). "An insight into additive manufacturing of fiber reinforced polymer composite," *International Journal of Lightweight Materials and Manufacture* 2(4), 267-278. DOI: 10.1016/j.ijlmm.2019.08.004

Article submitted: September 10, 2024; Peer review completed: October 13, 2024;  
Revised version received: October 29, 2024; Accepted: November 1, 2024; Published:  
November 13, 2024.

DOI: 10.15376/biores.20.1.331-356